

1 *Communication*

2 **Probing Synergies between Lignin rich and Cellulose** 3 **Compounds for Gasification**

4 **Martin J. Taylor,^{1,2} Apostolos K. Michopoulos,³ Anastasia A. Zabaniotou⁴ and Vasiliki**
5 **Skoulou^{1,2*}**

6 ¹ Energy and Environment Institute, University of Hull, Cottingham Road, Hull, HU6 7RX, United Kingdom

7 ² B³ Challenge Group, Department of Chemical Engineering, University of Hull, Cottingham Road, Hull
8 HU6 7RX, United Kingdom

9 ³ Energy and Environmental Design of Buildings Research Lab, University of Cyprus, P.O. Box 20537, 1678
10 Nicosia, Cyprus

11 ⁴ Department of Chemical Engineering, Aristotle University of Thessaloniki, P.O. Box 455, GR 541 24,
12 Thessaloniki, Greece

13 * Correspondence: V.Skoulou@hull.ac.uk

14 Received: date; Accepted: date; Published: date

15 **Abstract:** The fixed bed gasification of lignin rich and deficient mixtures was carried out to probe
16 the synergistic effects between two model compounds, Lignin Pink (LP) rich in Na and Cellulose
17 Microcrystalline (CM). Reaction conditions utilized the most commonly used air ratios in current
18 wood gasifiers at 750 °C and 850 °C. It was found that by increasing the lignin content in the mixture,
19 there was a selectivity change from solid to gas products, contrary to a similar study previously
20 carried out for pyrolysis. This change in product mix was promoted by the catalytic effect of Na
21 edge recession deposits on the surface of the char. As a result, the water gas shift reaction was
22 enhanced at 850 °C for the LP₄₈CM₅₂ mixture across all air ratios, this was evidenced by a strong
23 correlation between the produced H₂ and CO_x. Meanwhile, by lowering the lignin content in the
24 mixtures, the reactivity of cellulose microcrystalline was found to generate more char at higher
25 temperature, similar to lignin mixtures when undergoing pyrolysis.

26 **Keywords:** Gasification, Lignocellulosic Biomass Waste, Lignin, Cellulose, Na promotion, Water
27 Gas Shift

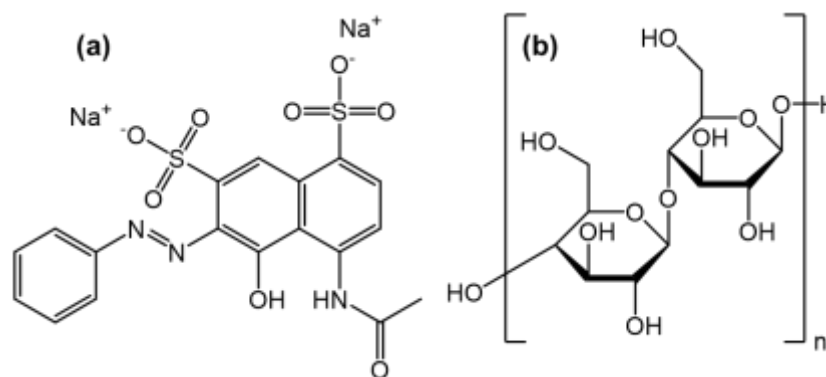
29 **1. Introduction**

30 The utilization of sustainable solid fuels such as woody wastes is one of many possible answers
31 to combat irreversible climate change damage, attributed to the extensive usage of fossil-based fuels
32 such as coal and the corresponding CO₂ emissions produced [1]. One method of replacing the
33 polluting coal, rich in mineral ash constituents, is the use of biorenewable feedstocks, specifically
34 lignocellulosic biomass wastes where upon the carbon cycle can be closed. This can be also done by
35 co-processing, or diluting the coal feed with other wastes such as pulps, pyrolysis tars or lignin rich
36 biorefinery sludges and even other biodegradable by-products. Here, the overall net CO₂ emissions
37 can be reduced to zero as a part of the natural carbon cycle, or even to negative if used in conjunction
38 with modern carbon capture technologies [2]. Currently, a popular feedstock used on a large scale
39 for bioenergy production are woody biomass residues, these are physically, chemically or
40 physicochemically pretreated [3,4] and fed into thermochemical reactors for pyrolysis (mainly solid
41 to liquid thermal cracking reactions) [5-7], gasification or combustion (mainly solid to gas, gas-gas
42 and thermochemical cracking reactions) [8,9]. However, variability of the lignocellulosic biomass
43 waste is a limiting factor in the use of large-scale waste reformation for the production of low carbon
44 energy [10]. This is due to wide variations in cellulose, hemicellulose and lignin ratios depending on
45 the feedstock (woody vs herbaceous). As a result, the chemical interactions and bonding brings in a
46 new paradigm as the feedstocks will each have differences in the required energy to thermally

47 decompose. Additionally, the presence and role of any inorganic ash constituents that may be present
48 in the substrate such as Na, K, S, Ca, Si, Mg or Cl must be considered. These elements form
49 compounds which can cause extensive damage to reactor systems, promote side reactions which
50 cause fouling, slagging and de-fluidization. Ultimately this leads to a breakdown in combustible fuel
51 gas production [11,12]. Additionally, inorganic components can catalyze the production of specific
52 gas products or produce toxic emissions in their own right such as H₂S or HCl [13,14].

53 Previously in 2018, work was published by Volpe, Zabaniotou and Skoulou whom found that
54 there is a synergistic effect between lignin and cellulose model compounds during pyrolysis [15]. It
55 was found that by varying the ratios between Lignin Pink and Cellulose Microcrystalline (**Figure 1**),
56 the thermochemical process outcome is altered. This is where increased lignin content alters the
57 reaction selectivity to generate more char. However, when compared to a 'real' feedstock such as
58 olive kernels or corn cobs the product mixtures are not the same. This is due to the feedstock
59 variability as mentioned previously which operates a wide range of thermochemical and tar thermal
60 cracking reactions that promote a different process due to an 'additive rule'. As a continuation of this
61 work, the model compounds underwent gasification across various temperatures and air ratio
62 (λ) values, where air ratio represents the ratio of the gasification air content to the total stoichiometric
63 air required for complete oxidization of a specific fuel. In line with our previously published work
64 [15], an assumption was made that various agro-residues of interest could be fairly resembled with
65 synthetic mixtures, composed only from cellulose and lignin. This is due to the relatively low
66 hemicellulose content which exists in both woody and herbaceous lignocellulosic waste. It was
67 assumed that the hemicellulose component would contribute a minor role during gasification due to
68 its similarities to cellulose [16].

69 This work demonstrates the effect of lignin and cellulose model compound wt% ratios on the
70 ratios of fuel gas species generated under varying gasification conditions, as well as the liquid and
71 solid products. The selected gasification conditions are the ones most commonly used in autothermal
72 industrial-scale woody biomass waste gasifiers [17]. Previously, for the pyrolysis of model compound
73 mixtures, it was found that the char yield was enhanced for lignin rich mixtures across all
74 temperatures, an inverse trend was shown for tar where cellulose rich mixtures were found to
75 produce a higher tar selectivity [15]. **Figure 1** as well as the ultimate analysis shown in our previous
76 work [15] show that the lignin model compound, Lignin Pink (LP), contains both Na and S, 8.7 wt%
77 and 12.6 wt%, respectively. However, this is contributing to less than <0.1 wt% ash content for the
78 lignin model compound [15]. The ash values observed for pure lignocellulosic biomass feedstocks
79 are very much higher, ranging in some cases >5 wt% [3]. Alternative waste feedstocks with higher
80 inorganic content are black liquor and pyrolysis oils as well as sludges produced during fossil fired
81 conventional energy generation [18]. It has previously been found that lignin thermochemical
82 decomposition, specifically char degradation can be promoted by Na [19]. This has been also shown
83 for the LP compound previously [20]. High Na content in a model compound is comparable to real
84 world feedstocks such as olive cake [21], olive wood [22], poplar bark [22] and fir mill residues [22].
85 It also exists in high concentrations in wheat straw [23] and buffalo gourd grass [22]. This behavior
86 means that Na present will force charring reactions leading to an increase in gaseous products [20].
87 As the temperature of gasification increases from 800 °C the rate of Na released into the gas phase
88 increases in a non-linear fashion. This is because Na released to the gas phase at lower temperatures
89 is transferred to the produced char forming channels in the carbon interface during gasification [24],
90 often forming larger mesopores than other alkali metals. This makes sodium, much like potassium
91 and calcium, edge-recession catalysts [24,25]. It has been shown in the past that the presence of Na
92 can effectively catalyze the water-gas shift reaction ($\text{CO} + \text{H}_2\text{O} \rightarrow \text{CO}_2 + \text{H}_2$), a mildly exothermic
93 reaction, boosting the production of CO₂ and H₂ [24]. Although seen as less active than K for
94 gasification, the Na present from the LP should provide a promotional effect on the gasification. The
95 presence of residual ash is appropriate for this model reaction as pretreatments for most
96 lignocellulosic waste feedstocks are not suitable at extracting all inorganics [3,11,12,26].



97

98

99

Figure 1 – Model lignocellulosic biomass waste probe molecules; (a) Lignin Pink and (b) Cellulose Microcrystalline, derived from an α -cellulose precursor

100 2. Materials and Methods

101 2.1 Sample Preparation and Characterization

102 Cellulose Microcrystalline (CM) and Lignin Pink (LP) were supplied by Sigma-Aldrich GmbH
 103 and Alfa Aesar U.S.A., respectively. In the same method mentioned previously [15], the LP and CM
 104 model compounds were thoroughly mixed in weight percentages of 17 wt% LP, 83 wt% CM
 105 (LP₁₇CM₈₃) to generate a lignin deficient material and 48 wt% LP, 52 wt% CM (LP₄₈CM₅₂) to resemble
 106 a material with a higher lignin content to mirror the composition of herbaceous and woody ‘real’
 107 feedstocks such as alfalfa, pine straw and flax fiber [27]. Individual proximate and ultimate analysis
 108 of the model compounds is presented in earlier work, where data was obtained from the supplier
 109 directly [15].

110 2.2 Gasification Experimental Study

111 Similarly, to the experimental setup described in more detail previously [15], the gasification of
 112 CM and LP (particle sizes $d_p = 100\text{--}200\ \mu\text{m}$) was carried out in a lab scale, downdraft fixed bed
 113 stainless steel batch atmospheric reactor under a controlled reactive atmosphere. Here, synthetic air
 114 (O_2 20% and N_2 80%) was diluted by a mass flow controller with nitrogen, to achieve the most
 115 commonly practiced gasification air ratios (λ) of 0.2, 0.3 and 0.4, to a flow rate of 20 mL/min,
 116 corresponding to ~ 0.4 s of gas residence time. The gasifier was heated to 750 °C and 850 °C, measured
 117 by a K-type thermocouple positioned in the sample holder of the reactor, the heating rate was
 118 calculated to be approximately 150 °C/min for a total reaction time of 20 min. Producer gas cleaning
 119 and subsequent sampling were carried out downstream from the reactor. Upon full gasification of
 120 the model compounds the reactor was cooled and disassembled to reclaim the char residue. The total
 121 tar yield including the aqueous phase was determined by subtraction of the produced gaseous and
 122 char products as illustrated by the overall general mass balance in **equation 1**.

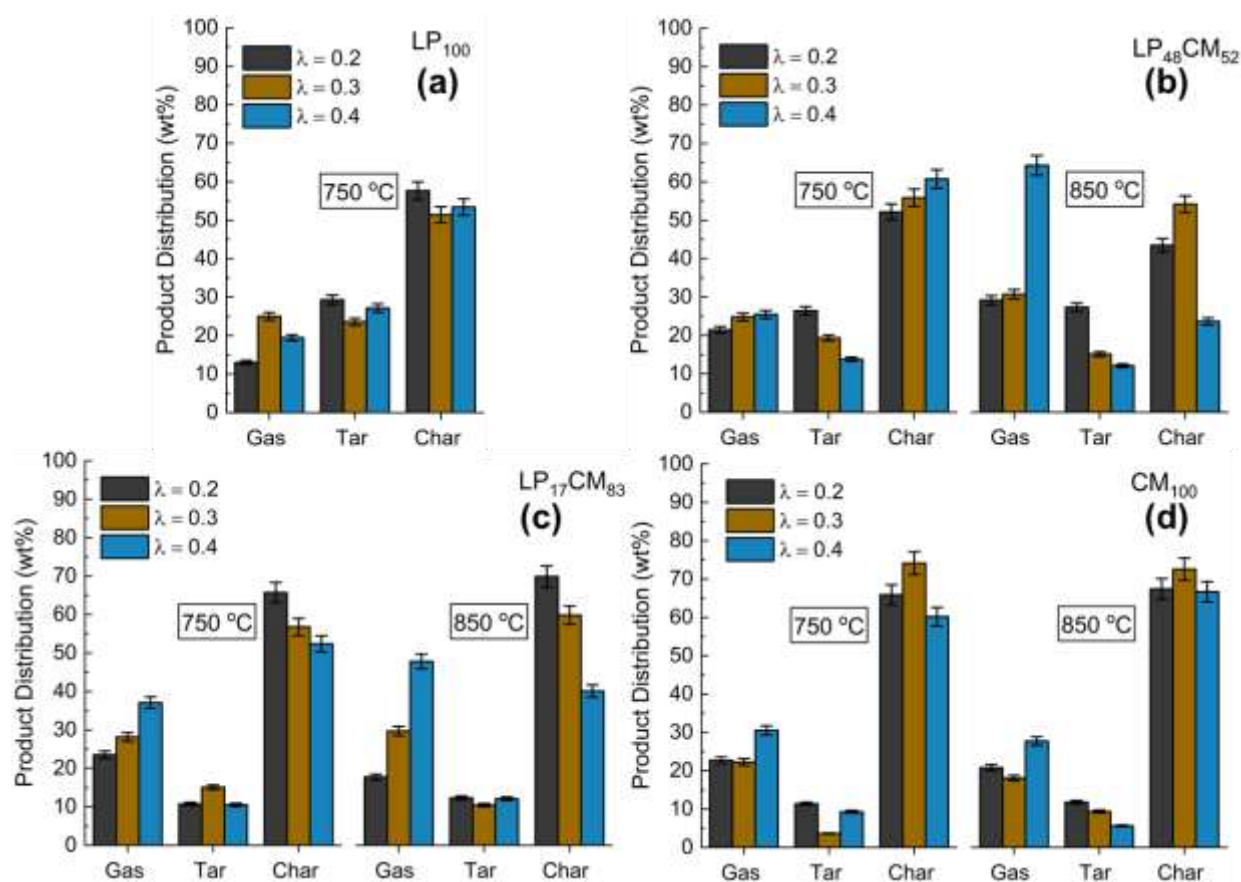
123 Eq 1 - Carbonaceous feedstock + Gasification medium (air) = Char + Gasification producer gas + Tar

124 The most common gas phase products were sampled via airtight gas sampling bags and
 125 analysed offline on an Agilent 6890N chromatograph fitted with two columns, HP-PlotQ and HP-
 126 Molsieve, with both an FID and TCD detectors. More details on the specific experimental systems
 127 can be found in previous published works by the authors [12,15,28].

128 3. Product Analysis and Discussion

129 **Figure 2a, b, c and d** show the product mix generated from the gasification with air of each of
 130 the model compound mixtures at two different temperatures (750 °C and 850 °C) and three different
 131 reaction atmospheres ($\lambda = 0.2, 0.3, 0.4$), corresponding to different under-stoichiometric air ratios and
 132 starting from the pure lignin (LP₁₀₀) in **Figure 2a** and decreasing, to a rich in lignin mixture, diluted
 133 with cellulose LP₄₈CM₅₂ (**Figure 2b**), a low lignin mixture LP₁₇CM₈₃ (**Figure 2c**) and the pure cellulose

134 CM₁₀₀ (Figure 2d). In our previous pyrolysis study, we found that the char yields were enhanced
 135 when using lignin rich mixtures [15]. However, in all cases (temperature and air ratio) for gasification
 136 this trend was not seen. In fact, the LP alone facilitated a far greater tar yield (Figure 2a) where it was
 137 found ~25-30 wt% of the product mix was tar based at $\lambda = 0.2$ and 0.3 conditions, corresponding to
 138 the high temperature pyrolytic stage of gasification. This might be attributed to the role of Na cations
 139 liberated during the thermal decomposition of the LP. Not only is the lignin decomposition pathway
 140 enhanced by Na, dehydration, demethoxylation (-OCH₃), decarboxylation (-COOH) reactions as well
 141 as char formation have been found previously to be catalyzed [29]. Although found to enhance
 142 various reactions, Na has been found to decrease the yield of organic volatiles and CO [29]. This has
 143 been echoed by Huang et al. who show that the reactivity of lignocellulosic chars increase with the
 144 addition/presence of metals, the order of promotion decreases down the following series,
 145 K > Na > Ca > Fe > Mg [30]. The major product intended from gasification are fuel gases, Figure 2b
 146 shows that by using the lignin rich LP₄₈CM₅₂ mixture at 850 °C there is a substantial selectivity change
 147 from char to gas, this is where over 64 wt% of the product mix was gas for an air ratio of $\lambda = 0.4$.
 148 Whereas for the same mixture at 750 °C under the same λ value there was only 25 wt% gas produced
 149 overall. It is clear from Figure 2a that overall, LP is responsible for low gas yields, as compared with
 150 mixtures and pure CM, Figure 2d, at 750 °C. By considering the gasification of the pure cellulose
 151 (CM₁₀₀) (Figure 2d) there was a maximum of 22.7 wt% gas produced. Although for the CM a
 152 maximum char yield, 74 wt%, could be obtained by using $\lambda = 0.3$ at 750 °C. With the exception of the
 153 pure lignin sample (LP₁₀₀), a maximum tar yield was generated for all mixtures in the lowest air ratio
 154 conditions ($\lambda = 0.2$), as was expected. It is clear that the gasification at conditions of higher λ ratio in
 155 the reactor promote char decomposition rather than restricting formation, especially at 850 °C
 156 (Figures 2b and 2c).



157

158

159

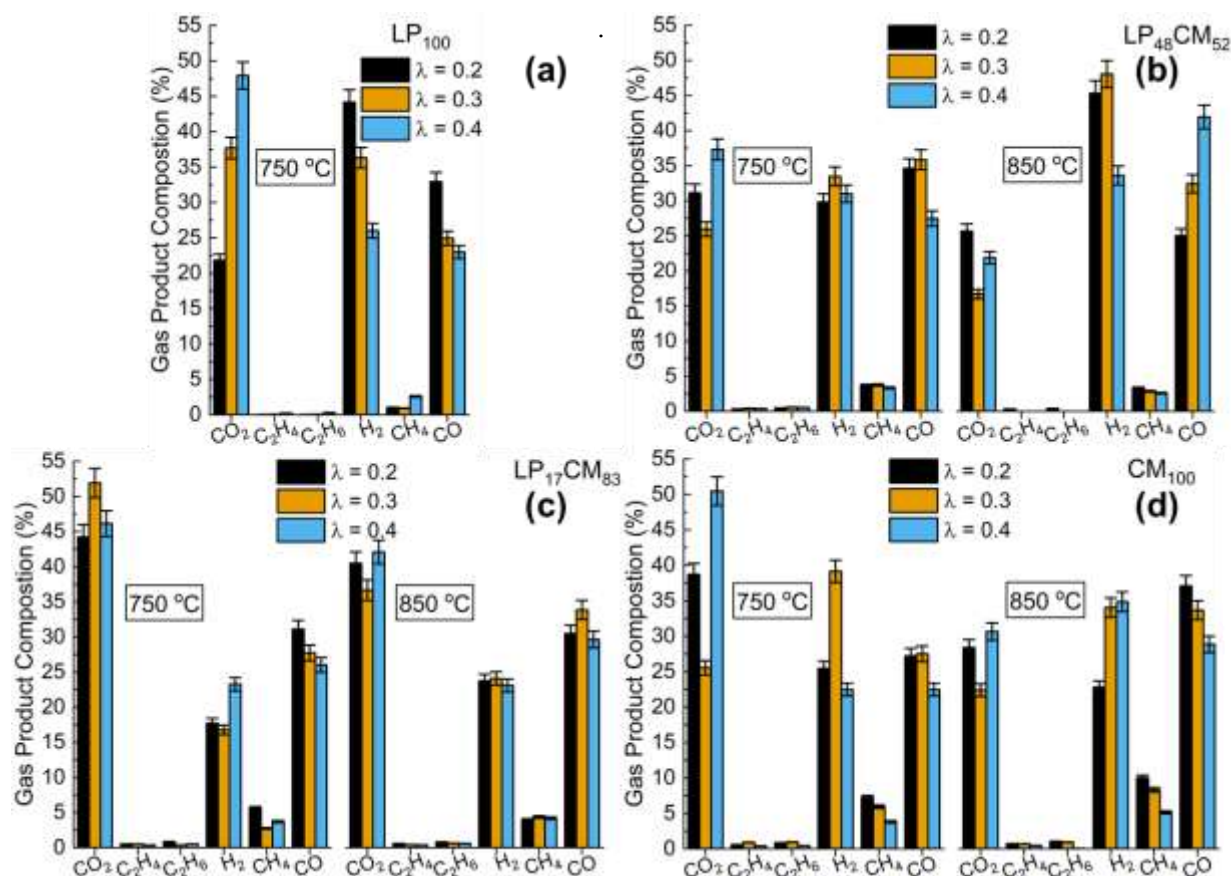
Figure 2 – Product distribution of; (a) LP₁₀₀, (b) LP₄₈CM₅₂, (c) LP₁₇CM₈₃ and (d) CM₁₀₀ at two different gasification temperature parameters, 750 °C and 850 °C. Air content in the flux is indicated by λ .

160 To determine the effect of reactant synergies, the gas product (normalized, excluding N₂)
161 selectivities have been presented in **Figures 3a-3d**, where **Figure 3a** is the undiluted LP₁₀₀ at 750 °C,
162 while in **Figure 3b** is LP₄₈CM₅₂, **Figure 3c** is LP₁₇CM₈₃ and **Figure 3d** is the undiluted CM₁₀₀ sample,
163 at both operational temperatures. For the low temperature gasification (750 °C) of LP under $\lambda = 0.2$,
164 far more H₂ and CO are formed as compared with the higher air ratio ($\lambda = 0.4$). This is where a
165 decrease of 41% and 30% was observed for H₂ and CO, respectively. As the O₂ concentration was
166 increased in the stream, the fuel gas selectivity drops significantly, favored by the richer oxygen
167 atmosphere and residual Na in the form of Na₂CO₃ decomposing to form CO₂. By diluting the lignin
168 content within the mixture, **Figure 3b** shows that the production of both CO and H₂ have been
169 increased dramatically at 850 °C. This data also shows that by increasing the air content, there is an
170 increase in the selectivity of CO opposed to CO₂, shown in **Figure 3a**. By mixing the two compounds
171 together there has been a profound decrease in CH₄ production (**Figure 3b** and **Figure 3c**) at both
172 temperatures, as compared with LP₁₀₀ (750 °C, $\lambda = 0.2$) and CM₁₀₀ (850 °C, $\lambda = 0.2$). For the low
173 temperature gasification of LP₁₇CM₈₃ (**Figure 3c**) there has been a large switch in selectivity towards
174 CO₂ across all λ values. At its maximum ($\lambda = 0.3$), 52% of the product mix was CO₂, for the same
175 reaction conditions this was 14.3% and 26.1% higher for LP₁₀₀ and LP₄₈CM₅₂, respectively. However,
176 the lower lignin containing mixture (**Figure 3c**) produces far less CO than LP₄₈CM₅₂ shown in **Figure**
177 **3b**. This mixture shows a true synergistic effect between both compounds as the H₂ and CO
178 production is far higher than LP₁₀₀ (**Figure 3a**) and CM₁₀₀ (**Figure 3d**) alone. **Figure 3d** does report the
179 highest selectivities towards ethylene (C₂H₄) and ethane (C₂H₆), 0.8% and 1.0% when operating at 850
180 °C and $\lambda = 0.2$. As the oxygen is increased in the stream the selectivities of these two molecules drops
181 to 0.5% and 0.1%, respectively. Interestingly this drop is only observed for LP₄₈CM₅₂ (**Figure 3b**)
182 where there is no production of ethylene or ethane. CM₁₀₀ when gasifying at 750 °C and $\lambda = 0.4$ was
183 found to possess more combustion characteristics, producing 50.4% of CO₂ (**Figure 3d**). Although
184 higher than LP₁₀₀ under the same conditions, both mixed materials were found to produce less CO₂
185 across both temperatures, at $\lambda = 0.4$. Overall, from **Figure 3** two general conclusions can be made: a)
186 the increase of gasification temperature leads to an increase in H₂ content in the producer gas. This is
187 due to the water-gas shift reaction and the hydrogen enriched gas mechanisms being temperature
188 dependent and commonly promoted at the industrial scale by alkali and alkaline-earth metal
189 catalysts, such as Na [31]. Also, hydrogen is liberated due to heavy volatiles cracking on the char
190 matrix [15,28]. Additionally, b) the effect of air ratio on the produced gasses is not directly connected
191 with the reduction of H₂ concentration, and/or the increase of CO_x.

192

193

194



195

196

197

198

Figure 3 – Gas phase product composition of; (a) LP₁₀₀, (b) LP₄₈CM₅₂, (c) LP₁₇CM₈₃ and (d) CM₁₀₀ at two different gasification temperature parameters, 750 °C and 850 °C. Air content in the flux is indicated by λ .

199

200

201

202

203

204

205

206

207

208

209

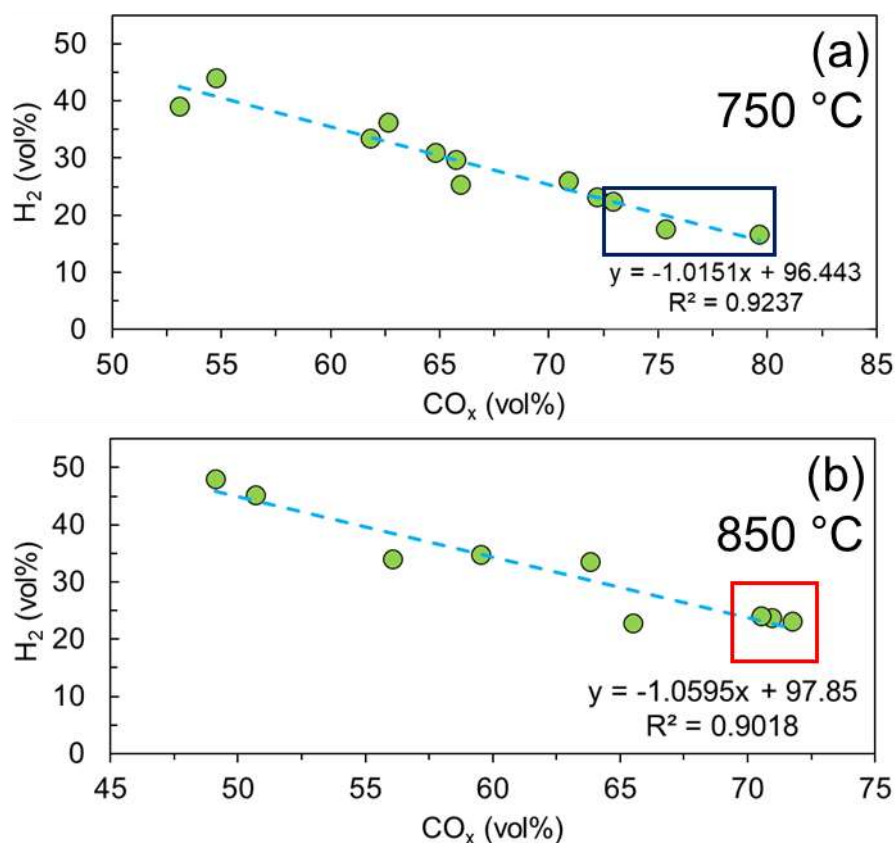
210

211

212

213

Figure 4a and **4b** illustrates the correlation between the H₂ content and the CO_x in the producer gas at 750 °C and 850 °C, respectively. It is worth noting that in both figures a strong linear correlation between H₂ and CO, CO₂ is noticed. More specifically the increase of carbon oxides (CO_x) in the producer gas decreases the production of H₂ and vice versa. **Figure 4a** shows that for LP₁₇CM₈₃ there is a greater concentration of CO_x molecules at 750 °C, across all air ratios (dark blue square). This is due to the greater char yields receiving a solid-gas reaction promotion from isolated Na deposits, donated by the LP. However, when operating at 850 °C there is not the same promotional effect observed for LP₁₇CM₈₃ but for the lignin rich mixture (LP₄₈CM₅₂) there is a substantial decrease in char yield. It is suspected that the Na rich deposits have enhanced the water-gas shift reaction, thermochemically decomposing the char with reactively formed steam. **Figure 4b** shows that this effect is shown across all three reactions, this means that the O₂ content is not important as an equilibrium has been reached (red square). The greater Na effect is assumed to be attributed to the decomposition of char (**Figure 2b**). As char is decreased, the CO evolved is readily reacted with produced steam in the reaction.



214

215 Figure 4 – Correlation between hydrogen and carbon oxides at two different gasification
 216 temperatures, a) 750 °C (dark blue square indicating LP₁₇CM₈₃) and b) 850 °C (red square indicating
 217 LP₄₈CM₅₂). For all experimental mixtures and conditions.

218 4. Conclusions

219 The gasification of the model compound mixtures containing Lignin Pink and Cellulose
 220 Microcrystalline took place under the most common varying oxygen containing atmospheres
 221 ($\lambda = 0.2, 0.3, 0.4$) and temperatures (750-850 °C) for current wood gasifiers. Here, varying ratios of the
 222 two compounds were used to examine the synergistic behavior between lignin and cellulose. An
 223 opposite trend was found to what was observed previously in our pyrolysis study, that char yields
 224 were enhanced when using lignin rich mixtures. For gasification it was found that CM rich mixtures
 225 produced more char, while lignin rich compounds produced a greater gas yield at 850 °C. It is
 226 believed that due to the catalytic activity of Na in gasification, specifically at higher air content. As
 227 the Na forms channels decorating the surface of the formed char, gas phase reactions are promoted,
 228 specifically through the water-gas shift reaction, where reactively formed steam interacts with the
 229 char. It was found that the lignin rich LP₄₈CM₅₂ mixture when operating at 850 °C provided the
 230 highest producer gas product mix. By increasing the Cellulose Microcrystalline content in the
 231 mixture, the oxidization process was accelerated where CO₂ was found to be the dominant product.
 232 In addition, a strong correlation between the produced H₂ and CO_x is observed. It was found that the
 233 Lignin Pink rich mixture received a substantial promotional effect from Na deposits decorating the
 234 surface of the char, enhancing the water-gas shift reaction and hydrogen enrichment mechanism
 235 when operating at 850 °C. As a result, the product mix was heavily pushed toward gas phase
 236 products opposed to charring reactions at 750 °C. The significance of the presented results enhance
 237 the existing literature with a series of experimental results useful for simulation, modelling and
 238 validation studies for the pyrolysis and or gasification of new era wastes. Examples of such are,
 239 feedstocks naturally high in Na, sludges from NaOH delignification processes and alkaline metal ion
 240 containing wastes from biorefineries.

241 **Author Contributions:** Conceptualization, V.S and A.Z; methodology, V.S; software, M.J.T; validation, M.J.T,
242 A.K.M and V.S; formal analysis, M.J.T, A.K.M and V.S; investigation, V.S and A.Z; resources, A.Z; data curation,
243 V.S; writing—original draft preparation, M.J.T; writing—review and editing, M.J.T, A.K.M and V.S;
244 visualization, A.K.M and V.S; supervision, A.Z and V.S; project administration, V.S; funding acquisition, V.S.

245 **Funding:** VS acknowledges partial funding from (IKY 2010, Greece), VS and MJT both acknowledge partial
246 funding from the EPSRC (EP/P034667/1) and the THYME project (UKRI, Research England).

247 **Acknowledgments:** Assoc. Prof. G. Stavropoulos (Aristotle University of Thessaloniki) for his support
248 providing both chemicals and the experimental rig.

249 **Conflicts of Interest:** The authors declare no conflict of interest.

250 References

- 251 1. Burnham, A.; Han, J.; Clark, C.E.; Wang, M.; Dunn, J.B.; Palou-Rivera, I. Life-cycle greenhouse gas
252 emissions of shale gas, natural gas, coal, and petroleum. *Environ Sci Technol* **2012**, *46*, 619-627,
253 doi:10.1021/es201942m.
- 254 2. Haszeldine, R.S. Carbon capture and storage: how green can black be? *Science* **2009**, *325*, 1647-1652,
255 doi:10.1126/science.1172246.
- 256 3. M. J. Taylor; H. A. Alabdrabalameer; V. Skoulou. Choosing Physical, Physicochemical and Chemical
257 Methods of Pre-Treating Lignocellulosic Wastes to Repurpose into Solid Fuels. *Sustainability* **2019**, *11*,
258 3604, doi:10.3390/su11133604.
- 259 4. Chen, H.Y.; Liu, J.B.; Chang, X.; Chen, D.M.; Xue, Y.; Liu, P.; Lin, H.L.; Han, S. A review on the
260 pretreatment of lignocellulose for high-value chemicals. *Fuel Processing Technology* **2017**, *160*, 196-206,
261 doi:10.1016/j.fuproc.2016.12.007.
- 262 5. Bahcivanji, L.; Gasco, G.; Paz-Ferreiro, J.; Mendez, A. The effect of post-pyrolysis treatment on waste
263 biomass derived hydrochar. *Waste Manag* **2020**, *106*, 55-61, doi:10.1016/j.wasman.2020.03.007.
- 264 6. Akubo, K.; Nahil, M.A.; Williams, P.T. Pyrolysis-catalytic steam reforming of agricultural biomass
265 wastes and biomass components for production of hydrogen/syngas. *Journal of the Energy Institute* **2019**,
266 *92*, 1987-1996, doi:10.1016/j.joei.2018.10.013.
- 267 7. Wyn, H.K.; Zárate, S.; Carrascal, J.; Yermán, L. A Novel Approach to the Production of Biochar with
268 Improved Fuel Characteristics from Biomass Waste. *Waste and Biomass Valorization* **2019**,
269 10.1007/s12649-019-00909-1, doi:10.1007/s12649-019-00909-1.
- 270 8. Wang, T.; Long, H.A. Techno-economic analysis of biomass/coal Co-gasification IGCC systems with
271 supercritical steam bottom cycle and carbon capture. *International Journal of Energy Research* **2014**, *38*,
272 1667-1692, doi:10.1002/er.3177.
- 273 9. Tarelho, L.A.C.; Neves, D.S.F.; Matos, M.A.A. Forest biomass waste combustion in a pilot-scale
274 bubbling fluidised bed combustor. *Biomass and Bioenergy* **2011**, *35*, 1511-1523,
275 doi:10.1016/j.biombioe.2010.12.052.
- 276 10. Liakakou, E.T.; Vreugdenhil, B.J.; Cerone, N.; Zimbardi, F.; Pinto, F.; André, R.; Marques, P.; Mata, R.;
277 Girio, F. Gasification of lignin-rich residues for the production of biofuels via syngas fermentation:
278 Comparison of gasification technologies. *Fuel* **2019**, *251*, 580-592, doi:10.1016/j.fuel.2019.04.081.
- 279 11. Taylor, M.J.; Alabdrabalameer, H.A.; Michopoulos, A.K.; Volpe, R.; Skoulou, V. Augmented Leaching
280 Pretreatments for Forest Wood Waste and Their Effect on Ash Composition and the Lignocellulosic
281 Network. *ACS Sustainable Chemistry & Engineering* **2020**, *8*, 5674-5682,
282 doi:10.1021/acssuschemeng.0c00351.

- 283 12. Vaskalis; Skoulou; Stavropoulos; Zabaniotou. Towards Circular Economy Solutions for The
284 Management of Rice Processing Residues to Bioenergy via Gasification. *Sustainability* **2019**, *11*,
285 doi:10.3390/su11226433.
- 286 13. de Lasa, H.; Salaices, E.; Mazumder, J.; Lucky, R. Catalytic steam gasification of biomass: catalysts,
287 thermodynamics and kinetics. *Chem Rev* **2011**, *111*, 5404-5433, doi:10.1021/cr200024w.
- 288 14. Kuramochi, H.; Wu, W.; Kawamoto, K. Prediction of the behaviors of HS and HCl during gasification
289 of selected residual biomass fuels by equilibrium calculation. *Fuel* **2005**, *84*, 377-387,
290 doi:10.1016/j.fuel.2004.09.009.
- 291 15. Volpe, R.; Zabaniotou, A.A.; Skoulou, V. Synergistic Effects between Lignin and Cellulose during
292 Pyrolysis of Agricultural Waste. *Energy & Fuels* **2018**, *32*, 8420-8430,
293 doi:10.1021/acs.energyfuels.8b00767.
- 294 16. Basu, P. *Biomass Gasification, Pyrolysis and Torrefaction: Practical Design and Theory*, Second ed.; Elsevier
295 Science: 2013.
- 296 17. Mevissen, N.; Schulzke, T.; Unger, C.A.; an Bhaird, S.M. Thermodynamics of autothermal wood
297 gasification. *Environmental Progress & Sustainable Energy* **2009**, *28*, 347-354, doi:10.1002/ep.10393.
- 298 18. Bach-Oller, A.; Furusjö, E.; Umeki, K. Fuel conversion characteristics of black liquor and pyrolysis oil
299 mixtures: Efficient gasification with inherent catalyst. *Biomass and Bioenergy* **2015**, *79*, 155-165,
300 doi:10.1016/j.biombioe.2015.04.008.
- 301 19. Fryda, L.A. Development of advanced power production systems with biomass utilization Doctoral
302 thesis, National Technical University of Athens Athens, 2006.
- 303 20. Shen, D.; Hu, J.; Xiao, R.; Zhang, H.; Li, S.; Gu, S. Online evolved gas analysis by Thermogravimetric-
304 Mass Spectroscopy for thermal decomposition of biomass and its components under different
305 atmospheres: part I. Lignin. *Bioresour Technol* **2013**, *130*, 449-456, doi:10.1016/j.biortech.2012.11.081.
- 306 21. Lapuerta, M.; Acosta, A.; Pazo, A. Fouling Deposits from Residual Biomass with High Sodium Content
307 in Power Plants. *Energy & Fuels* **2015**, *29*, 5007-5017, doi:10.1021/acs.energyfuels.5b00356.
- 308 22. Vassilev, S.V.; Baxter, D.; Andersen, L.K.; Vassileva, C.G. An overview of the chemical composition of
309 biomass. *Fuel* **2010**, *89*, 913-933, doi:10.1016/j.fuel.2009.10.022.
- 310 23. Xue, Z.; Zhong, Z.; Lai, X. Investigation on gaseous pollutants emissions during co-combustion of coal
311 and wheat straw in a fluidized bed combustor. *Chemosphere* **2020**, *240*, 124853,
312 doi:10.1016/j.chemosphere.2019.124853.
- 313 24. Arnold, R.A.; Hill, J.M. Catalysts for gasification: a review. *Sustain Energy Fuels* **2019**, *3*, 656-672,
314 doi:10.1039/c8se00614h.
- 315 25. Baker, R.T.K.; Chludzinski, J.J. Catalytic Gasification of Graphite by Calcium and Nickel Calcium.
316 *Carbon* **1985**, *23*, 635-644, doi:Doi 10.1016/0008-6223(85)90223-4.
- 317 26. Saidur, R.; Abdelaziz, E.A.; Demirbas, A.; Hossain, M.S.; Mekhilef, S. A review on biomass as a fuel for
318 boilers. *Renewable and Sustainable Energy Reviews* **2011**, *15*, 2262-2289, doi:10.1016/j.rser.2011.02.015.
- 319 27. Watkins, D.; Nuruddin, M.; Hosur, M.; Tcherbi-Narteh, A.; Jeelani, S. Extraction and characterization
320 of lignin from different biomass resources. *Journal of Materials Research and Technology* **2015**, *4*, 26-32,
321 doi:10.1016/j.jmrt.2014.10.009.
- 322 28. Skoulou, V.; Zabaniotou, A.; Stavropoulos, G.; Sakelaropoulos, G. Syngas production from olive tree
323 cuttings and olive kernels in a downdraft fixed-bed gasifier. *International Journal of Hydrogen Energy*
324 **2008**, *33*, 1185-1194, doi:10.1016/j.ijhydene.2007.12.051.

- 325 29. Jakab, E.; Faix, O.; Till, F.; Szekely, T. The Effect of Cations on the Thermal-Decomposition of Lignins.
326 *Journal of Analytical and Applied Pyrolysis* **1993**, *25*, 185-194, doi:Doi 10.1016/0165-2370(93)80039-3.
- 327 30. Huang, Y.; Yin, X.; Wu, C.; Wang, C.; Xie, J.; Zhou, Z.; Ma, L.; Li, H. Effects of metal catalysts on CO₂
328 gasification reactivity of biomass char. *Biotechnology advances* **2009**, *27*, 568-572,
329 doi:10.1016/j.biotechadv.2009.04.013.
- 330 31. Ebadi, A.G.; Hisoriev, H.; Zarnegar, M.; Ahmadi, H. Hydrogen and syngas production by catalytic
331 gasification of algal biomass (*Cladophora glomerata* L.) using alkali and alkaline-earth metals
332 compounds. *Environ Technol* **2019**, *40*, 1178-1184, doi:10.1080/09593330.2017.1417495.

333



© 2020 by the authors. Submitted for possible open access publication under the terms and conditions of the Creative Commons Attribution (CC BY) license (<http://creativecommons.org/licenses/by/4.0/>).

334